15/01/2017
Biotechnology and Bioengineering

Functional expression of aryl-alcohol oxidase in *Saccharomyces cerevisiae* and *Pichia pastoris* by directed evolution

Javier Viña-Gonzalez[1], Katarina Elbl[1], Xavier Ponte[2], Francisco Valero[2] and Miguel Alcalde[1]*

[1]Department of Biocatalysis, Institute of Catalysis, CSIC, Cantoblanco, 28049 Madrid, Spain.

[2]Departamento de Ingeniería Química, Biológica y Medioambiental, Escuela de Ingeniería, Universidad Autónoma de Barcelona, Bellaterra, 08193 Barcelona, Spain.

*Corresponding author: malcalde@icp.csic.es

Running title: A tandem-yeast expression system for aryl-alcohol oxidase.

Keywords: Directed evolution, aryl-alcohol oxidase, functional expression, *Saccharomyces cerevisiae*, *Pichia pastoris,* bioreactor.

ABSTRACT

Aryl-alcohol oxidase (AAO) plays a fundamental role in the fungal ligninolytic secretome, acting as a supplier of H_2O_2. Despite its highly selective mechanism of action, the presence of this flavooxidase in different biotechnological settings has hitherto been hampered by the lack of appropriate heterologous expression systems. We recently described the functional expression of the AAO from *Pleurotus eryngii* in *Saccharomyces cerevisiae* by fusing a chimeric signal peptide (preαproK) and applying structure-guided evolution. Here, we have obtained an AAO secretion variant that is readily expressed in *S. cerevisiae* and overproduced in *Pichia pastoris*. First, the functional expression of AAO in *S. cerevisiae* was enhanced through the in vivo shuffling of a panel of secretion variants, followed by the focused evolution of the preαproK peptide. The outcome of this evolutionary campaign -an expression variant that accumulated 4 mutations in the chimeric signal peptide, plus two mutations in the mature protein- showed 350-fold improved secretion (4.5 mg/L) and was stable. This secretion mutant was cloned into *P. pastoris* and fermented in a fed-batch bioreactor to enhance production to 25 mg/L. While both recombinant AAO from *S. cerevisiae* and *P. pastoris* were subjected to similar N-terminal processing and had a similar pH activity profile, they differed in their kinetic parameters and thermostability. The strong glycosylation observed in the evolved AAO from *S. cerevisiae* underpinned this effect, since when the mutant was produced in the glycosylation-deficient *S. cerevisiae* strain Δ*kre2*, its kinetic parameters and thermostability were comparable to its poorly glycosylated *P. pastoris* recombinant counterpart.

1. INTRODUCTION

Aryl-alcohol oxidase (AAO, EC.1.1.3.7) is a monomeric extracellular flavoprotein that oxidizes a wide range of aromatic alcohols to their corresponding carbonyl compounds, concomitantly releasing H_2O_2. As a member of the glucose-methanol-choline (GMC) oxidoreductase superfamily, this FAD-dependent enzyme is secreted by different basidiomycetes involved in natural wood decay. The main role of AAO in nature is to supply ligninolytic peroxidases with H_2O_2, as well as to switch on the Fenton reaction in the combustion of lignin (Ferreira et al., 2005; Hernandez-Ortega et al., 2012a). In terms of biotechnological settings, AAO could be used in lignocellulose biorefineries to produce 2nd generation biofuels and added-value chemicals (Martinez et al., 2009; Alcalde, 2015). Moreover, and thanks to a highly enantioselective mechanism, AAO becomes very attractive for the chiral resolution of secondary alcohols aimed at obtaining valuable building blocks for pharmaceutical processes (Hernandez-Ortega et al., 2012b). Along these lines, recent findings highlight the oxidative potential of this enzyme with renewal chemicals, such as furfural derivatives for the (bio)polymer industry (Carro et al., 2015; Martinez et al., 2017). Despite these promising features, the lack of suitable heterologous functional expression systems in which the properties of AAO can be sculptured by directed evolution has precluded the use of this versatile flavooxidase in different industrial applications. We previously reported the initial functional expression of AAO from the white-rot fungus *Pleurotus eryngii* in *Saccharomyces cerevisiae* (Viña-Gonzalez et al., 2015). This was achieved by designing a chimeric signal peptide (preαproK) that fused the pre- and pro-region of the α-factor and the K_1 killer toxin prepro-leaders from *S. cerevisiae*, and subsequently employing directed evolution to restricted AAO regions. We obtained a panel of AAO secretion variants that was led by the $_{Sac}$FX7 mutant, in which the consensus/ancestral substitution (H91N) was responsible for a ~100-fold improvement in total activity, as well as enhanced stability in terms of temperature and pH.

The current work describes a tandem-yeast expression system for AAO that links the directed evolution for secretion in *S. cerevisiae* to its over-production in *Pichia pastoris* on a bench-bioreactor scale. Harnessing the high frequency of homologous DNA recombination of *S. cerevisiae*, mutant libraries were constructed by shuffling $_{Sac}$FX7 with an ensemble of AAO secretion variants, while the chimeric peptide was further subjected to independent mutational loading. The resulting evolved AAO was transferred to *P. pastoris* for overproduction in a fed-batch bioreactor and characterized biochemically. To shed light on the effects exerted by hyperglycosylation in *S. cerevisiae*, the recombinant variant expressed in *P. pastoris* was further benchmarked with its counterpart secreted by a glycosylation-deficient *S. cerevisiae* strain.

2. MATERIAL AND METHODS

2.1 Strains and chemicals

All chemical were reagent-grade purity. Basal salts, PTM1 salts, *p*-methoxybenzyl alcohol, ABTS (2,2'-azino-bis(3-ethylbenzothiazoline-6-sulphonic acid)), horseradish peroxidase (HRP), Taq polymerase and the Yeast Transformation Kit were purchased from Sigma-Aldrich (SaintLouis, MO, USA). Zymoprep Yeast Plasmid Miniprep, Yeast Plasmid Miniprep Kit I and Zymoclean Gel DNA Recovery Kit were from Zymo Research (Orange, CA, USA). The *P. pastoris* expression vector (pPICZ B), the *P. pastoris* strain X-33 and zeocin were purchased from Invitrogen (Carlsbad, CA, USA). The protease deficient *S. cerevisiae strain* BJ5465 (α ura3-52 trp1 leu2Δ1 his3Δ200 pep4::HIS3 prb1Δ1.6R can1 GAL) was from LGC Promochem (Barcelona, Spain) whereas the glycosylation deficient *S. cerevisiae strain* YDR483W BY4742 (MATalpha his3delta1 leu2delta0 lys2delta0 ura3delta0 deltaKRE2) was from ATCC (Manassas, VA, USA). The *Escherichia coli* strainXL2-Blue competent cells and Phusion DNA Polymerase were obtained from Agilent Technologies (Santa Clara, CA, USA). Restriction endonucleases BsaI, XhoI, XbaI, KpnI, PmeI, the DNA Ligation Kit, the Antarctic phosphatase, EndoH and T4 DNA

Ligase were purchased from New England Biolabs (Ipswich, MA, USA). Oligonucleotide primers were acquired from Isogen Life Science (Barcelona, Spain).

2.2 Culture media

2.2.1 Culture media for *Saccharomyces cerevisiae*

Minimal medium contained 0.67% (w:v) yeast nitrogen base, 1.92 g/L yeast synthetic drop-out medium supplement without uracil, 2% (w:v) raffinose and 25 µg/mL chloramphenicol. SC drop-out plates contained 0.67% (w:v) yeast nitrogen base, 1.92 g/L yeast synthetic drop-out medium supplement without uracil, 2% (w:v) bacto agar, 2% (w:v) D-glucose and 25 µg/mL chloramphenicol. YP medium contained 10 g yeast extract, 20 g peptone and double-distilled H_2O (ddH_2O) to 650 mL. Expression medium contained 144 mL YP 1.55x, 13.4 mL 1M KH_2PO_4 pH 6.0 buffer, 22.2 mL 20% galactose (w:v), 0.222 mL 25 µg/mL chloramphenicol and ddH_2O to 200 mL.

2.2.2 Culture media for *Pichia pastoris*

YPD medium contained 10 g/L yeast extract, 20 g/L peptone, 4 g/L D-glucose and 25 µg/mL zeocin whereas YPD plates also contained 2% (w:v) bacto agar. BMD1 medium contained 100 mM potassium phosphate buffer pH 6.0, 3.5 g/L yeast nitrogen base without amino acids, 400 µg/L biotin and 10 g/L D-glucose. BMM2 medium contained 100 mM potassium phosphate buffer pH 6.0, 3.5 g/L yeast nitrogen base without amino acids, 400 µg/L biotin and 2% methanol (v:v). BMM10 medium contained 100 mM potassium phosphate buffer pH 6.0, 3.5 g/L yeast nitrogen base without amino acids, 400 µg/L biotin and 10% methanol (v:v). BMMY medium contained 100 mM potassium phosphate buffer pH 6.0, 3.5 g/L yeast nitrogen base without amino acids, 400 µg/L biotin and 0.5% methanol (v:v). Basal salts medium contained 26.7 mL/L 85% phosphoric acid, 0.93 g/L $CaSO_4 \cdot 2H_2O$, 14.9 g/L $MgSO_4 \cdot 7H_2O$, 18.2 g/L K_2SO_4, 4.13 g/L KOH and 40 g/L glycerol.

2.2.3 Culture media for *Escherichia coli*

Luria-Bertani (LB) medium contained 10 g NaCl, 5 g yeast extract, 10 g peptone, 1 mL 100 mg/mL ampicillin and ddH_2O to 1 L whereas LB agar plates also contained 2% (w:v) bacto agar.

2.3. Laboratory evolution

2.3.1 In vivo shuffling

PCR reactions were performed separately with mutants $_{Sac}$FX7, $_{Sac}$13H2, $_{Sac}$10G5, $_{Sac}$7A11, $_{Sac}$4C7 and $_{Sac}$12G12. Reaction mixtures were prepared in a final volume of 50 µL containing DNA template (0.92 ng/µL), 90 nM oligo sense RMLN (5'-CCTCTATACTTTAACGTCAAGG-3'), 90 nM Reverse primer RMLC (5'-GGGAGGGCGTGAATGTAAGC-3'), 0.3 mM dNTPs (0.075 mM each), 3% (v:v) dimethylsulfoxide (DMSO), 1.5 mM $MgCl_2$, increasing concentrations of $MnCl_2$ (0.025, 0.05, 0.1 mM) and 0.05 U/µL Taq DNA polymerase. PCRs were performed in a thermocycler (Mycycler, Bio-Rad,Hercules, CA, USA) and parameters were: 95°C for 2 min (1 cycle); 95°C for 45 s, 50°C for 45 s, 74°C for 45 s (28 cycles); and 74°C for 10 min (1 cycle). The PCR products were mixed with the linearized episomal shuttle vector pJRoC30 (at a PCR product/linearized plasmid ratio of 6:1) and transformed into competent *S. cerevisiae* cells to promote in vivo DNA shuffling. The whole gene was reassembled in vivo by transformation into *S. cerevisiae*, a process facilitated by the design of ~50-bp overhangs flanking each recombination area. Transformed cells were plated on SC drop-out plates and incubated for 3 days at 30°C. Colonies containing the whole autonomously replicating vector were picked and subjected to high-throughput screening.

2.3.2 MORPHING library at the preαproK

The preαproK signal peptide of $_{Sac}$FX8 variant (261 bp) was used as DNA template for focused random mutagenesis technique MORPHING (Mutagenic Organized Recombination Process by Homologous IN vivo Grouping) (Gonzalez-Perez et al., 2014). Mutagenic PCR was prepared in a final volume of 50 µL containing: 90 nM RMLN, 90 nM C-ter prokiller (5´-

ACGCTTGGCCACTGCTGGAAT-3'), 0.3 mM dNTPs (0.075 mM each), 3% DMSO, 0.1 mM $MnCl_2$, 1.5 mM $MgCl_2$, 0.05 U/µL l Taq polymerase DNA, and 0.92 ng/µL template. The amplification parameters were 95°C for 2 min (1 cycle); 94°C for 45 s, 50°C for 45 s, and 74°C for 30 s (28 cycles); and 74°C for 10 min (1 cycle). The whole AAO gene (1701 bp) was amplified by high-fidelity PCR in a final volume of 50 µL containing: 250 nM oligo sense N-ter AAO (5'-GCCGATTTTGACTACGTTGTCGTCG-3'), 250 nM oligo antisense RMLC, 1 mM dNTPs (0.25 mM each), 3% DMSO, 0.05 U/µL Phusion DNA polymerase, and 2 ng/µL template. High-fidelity PCR was performed using the following parameters: 95°C for 2 min (1 cycle); 94°C for 30 s, 50°C for 30 s, 74°C for 2 min (30 cycles); and 74°C for 10 min (1 cycle). PCR products were mixed in equimolar amounts, 200 ng mutagenic signal peptide and 200 ng mature non-mutagenized protein, and transformed with linearized pJRoC30 (200 ng) into chemically competent cells, as described above.

2.3.3 High-throughput screening (HTS) assay

Individual clones were picked and cultured in sterile 96-well plates containing 50 µL of minimal medium. In each plate, column number 6 was inoculated with the parental type (internal standard) and well H1 with URA3- *S. cerevisiae* cells (negative control). Plates were sealed to prevent evaporation and incubated at 30°C, 225 rpm and 80% relative humidity in a humidity shaker (Minitron-INFORS, INFORS-HT, Switzerland). After 48 hours, 160 µL of expression medium were added to each well and cultured for additional 48 hours. Aliquots of 20 µL of yeast supernatants were transferred to a 96-well plate with liquid handler robotic station Freedom EVO (Tecan, Männedorf, Switzerland) and 180 µL of HRP-ABTS reagent (final concentrations of HRP-ABTS reagent in the well: 1mM *p*-methoxybenzyl alcohol, 2.5 mM ABTS, 1µg/mL HRP in 100 mM phosphate buffer pH 6.0) were dispensed with Multidrop™ Combi Reagent Dispenser (Thermo Scientific, Massachusetts, USA). The plates were incubated at room temperature and measured in kinetic mode at 418nm ($\varepsilon ABTS^{\bullet+}$ = 36000 M^{-1} cm^{-1}). The

HTS-assay incorporated two consecutive re-screenings to rule out the selection of false positives as described elsewhere (Viña-Gonzalez et al., 2016).

2.4 AAO in *S. cerevisiae*

2.4.1 Shake-flask fermentation

A single colony from the *S. cerevisiae* clone containing the AAO fusion gene was picked from a SC drop-out plate, inoculated in minimal medium (20 mL) and incubated for 48 h at 30°C and 220 rpm. An aliquot of cells was removed and used to inoculate minimal medium (100 mL) in a 500 mL flask (OD_{600} = 0.25). The cells completed two growth phases (6–8 h; OD_{600} = 1) and then expression medium (900 mL) was inoculated with the pre-culture (100 mL) (OD_{600} of 0.1). After incubating for 72 h at 25°C and 220 rpm (maximal AAO activity; OD_{600} = 25–30), the cells were recovered by centrifugation at 4500 rpm and 4°C (Avanti J-E centrifuge, Beckman Coulter Inc. CA, USA) and the supernatant was double-filtered (using both glass membrane filter and a nitrocellulose membrane of 0.45 µm pore size). The incubation for the expression in glycosylation deficient *S. cerevisiae* strain YDR483W BY4742 was stopped after 18 h to avoid proteolytic degradation of the AAO by extracellular yeast proteases.

2.5 AAO in *P. pastoris*

2.5.1 AAO cloning in *P. pastoris*

The coding region of the evolved AAO variant (1962 bp) was cloned into the expression vector pPICZ-B. First, pJRoC30-FX7/FX9 was used to amplify AAO variants with the primers ppKpnAAO-dir (5´- GGGGTACCATGAGATTTCCTTCAATTTTACTGC-3´) and ppAAO-rev (5´-GCTCTAGACTACTGATCAGCCTTGATAAGATCGGC-3´), the primers included targets for restriction enzymes KpnI and XbaI, respectively (underlined). The PCR reactions were prepared in a final volume of 50 µL containing 250 nM of each primer, 1 mM dNTPs (0.25 mM each), 3% DMSO, 0.05 U/µL Phusion DNA polymerase, and 2 ng/µL template. The parameters for the PCR were: 95°C for 2 min (1 cycle); 94°C for 30 s, 50°C for 30 s, 74°C for 2 min (30 cycles); and 74°C

for 10 min (1 cycle). The pPICZ-B vector and the PCR product were digested with the restriction enzymes KpnI and XbaI at 37°C for 1 h. The 5´ and 3´ends of the linearized pPICZ-B plasmid were dephosphorylated using antarctic phosphatase at 37°C for 1 h adding 1 U of enzyme per every 200 ng of linearized vector. The PCR product and the linearized vector were loaded onto a preparative agarose gel, purified using the Zymoclean Gel DNA Recovery kit and ligated with T4 DNA ligase at room temperature for 30 min. After transformation of the pPICZ-B-AAO construct into chemically competent *E. coli* XL2-Blue cells, the plasmid was proliferated, linearized with the restriction enzyme PmeI at 37°C for 1 h and transformed into electro-competent *P. pastoris* X-33 cells. Electro-competent *P. pastoris* cells were prepared and transformed with the construction as described in the protocol from Lin-Cereghino et al. (Lin-Cereghino et al., 2000) mixing 200 ng of linearized vector and 50 µL of competent cells. Transformants were grown on YPD plates.

2.5.2 Deep-well plate fermentation

P. pastoris colonies containing AAO under the control of the AOX1 promoter (pPICZ-B-AAO) were picked and cultivated in 96-deep-well plates containing 300 µL of BMD1 medium per well. The plates were incubated at 25°C, 300 rpm and 80% humidity for 2 days in a humidity shaker. Afterwards, 300 µL of BMM2 medium were added per well. After 12 hours of incubation, 70 µL of BMM10 medium were added to each well repeating this addition every 24 hours for 3 days. After 142 h, the activity with *p*-methoxybenzyl alcohol was measured (final concentrations in the reaction mixture: 1mM *p*-methoxybenzyl alcohol, 2.5 mM ABTS, 1µg/mL HRP in 100 mM phosphate buffer pH 6.0).

2.5.3 Shake-flask fermentation

Transformants with the best activity from the deep-well plate fermentations were grown in YPD agar plates and inoculated in 3 mL of liquid YPD at 30°C and 250 rpm. The culture reached the optical density at 600 nm at 1 after 6–7 h and was inoculated in 20 mL of BMMY

medium in 100 mL shaken flasks. The cultures were incubated at 25°C or 30°C and they were supplemented with 250 µL of methanol every 24 h. After 3 days of methanol addition, the best clone with the highest activity was selected for the bioreactor fermentation.

2.5.4 Production in Bioreactor

The FX9 mutant ($_{\pi}$FX9) under the control of the AOX1 promoter in the pPICZ-B-FX9 construct was produced in a 5 L vessel fermenter (Minifors, INFORS-HT, Switzerland). The bioreactor was filled with 2 L of basal salts medium (initial volume: 2 L). After sterilization, 4.35 mL/L PTM1 trace salts and 1 mL Antifoam 204 were added to the medium and the pH was adjusted with ammonium hydroxide to 5.0. The fermentation was started with the addition of 0.2 L of preculture grown on YPD medium in several baffled shaken flasks at 150 rpm and 30°C overnight (OD_{600} between 6–10). According to the *Pichia Fermentation Process Guidelines* of Invitrogen the batch fermentation was run at 30°C, 600 rpm and air aeration 1 vvm. Once all the glycerol from the batch was consumed, the glycerol fed phase was initiated by the addition of 50 % (w/v) glycerol feed containing 12mL/L PTM1 trace salts to achieve higher cell density at a 21.8 mL/h feed rate. After 2 h, the glycerol feed faded out by a linear ramp 14.6-0 mL/h over 2 h and the methanol feed containing 12 mL/L PTM1 trace salts started at a 7.2 mL h^{-1} for the culture to transition and adapt to methanol. From this time on the temperature was set to 25°C and the Dissolved Oxygen (DO) above 20% with the control of the stirring speed between 600 and 1200 rpm and aeration using mixtures of air and O_2 within 0.7 and 1 vvm. At the end of the transition phase the methanol/PTM1 feeding was increased to 14.6 mL/h until the end of the process. Water evaporation losses were minimized during the process with an exhaust gas condenser and cooling water at 4°C. The fermentation was controlled by taking samples for biomass analysis and AAO activity: The cell concentration was monitored by measuring the optical density of cultures at 600 nm (OD_{600}). For wet dry weight (CDW) measurement, cells were separated from 1 mL culture broth by centrifugation at 10,000 g for 5 minutes using pre-weighed 1.5 mL tubes. The wet weight is measured immediately after all the yeast

supernatant has been removed. AAO activity was measured with HRP/ABTS method with *p*-methoxybenzyl alcohol as the substrate.

2.6 AAO purification

The FX9 variants expressed in *S. cerevisiae* (protease deficient strain BJ5465 and glycosylation deficient strain YDR483W BY4742) and *P. pastoris* were purified to homogeneity as described in a former work (Viña-Gonzalez et al., 2015).

2.7 AAO biochemical characterization

2.7.1 N-terminal analysis and pI Determination

Purified AAO variants were subjected to SDS/PAGE, and the protein band was blotted onto PVDF membranes. The PVDF membrane was stained with Coomassie Brilliant Blue R-250, after which the enzyme band was excised and processed for N-terminal amino acid sequencing on a precise sequencer at the Protein Chemistry Service at the The Biological Research Center (Madrid, Spain). Purified FX9 (8 µg) was subjected to two-dimensional electrophoresis gel in order to determine the pI.

2.7.2 Determination of kinetic-thermostability (T_{50})

Appropriate dilutions of AAO were prepared for the assay. The gradient scale ranging from 30 to 80°C was established as follows: 30.0, 31.4, 34.8, 39.3, 45.3, 49.9, 53, 55, 56.8, 59.9, 64.3, 70.3, 75, 78.1 and 80°C. This gradient profile was achieved using a thermocycler. After 10 min of incubation, AAO samples were removed and chilled out on ice for 10 min and incubated further at room temperature for 5 min. Finally, samples of 20 µL were added to 180 µL volumes of 100 mM sodium phosphate pH 6.0 buffer containing 1mM *p*-methoxybenzyl alcohol and activity was measured as anisaldehyde production as absorption at 285 nm (ε_{285} = 16,950 M^{-1} cm^{-1}). Thermostability values were calculated from the ratio between the residual activities incubated at different temperature points and the initial activity at room temperature. The T_{50} value was determined by the transition midpoint of the inactivation

curve of the protein as a function of temperature, which in our case was defined as the temperature at which the enzyme lost 50% of its activity following an incubation of 10 minutes. All reactions were performed by triplicate.

2.7.3 pH activity profile

Appropriate dilutions of enzyme samples were prepared in such a way that aliquots of 20 µL gave rise to a linear response in kinetic mode. The optimum pH activity was determined using 100 mM citrate-phosphate-borate buffer at different pH values (2.0, 3.0, 4.0, 5.0, 6.0, 7.0, 8.0 and 9.0) containing 0.3 *p*-methoxybenzyl alcohol.

2.7.4 Kinetic parameters

Kinetic constants for AAO were estimated in 100 mM sodium phosphate pH 6.0. Reactions were performed by triplicate and substrates oxidations were followed by measuring the absorption at 285 nm for *p*-methoxybenzyl alcohol, ε_{285} = 16,950 M^{-1} cm^{-1}; 310 nm for veratryl alcohol, ε_{310} = 9,300 M^{-1} cm^{-1}; 250 nm for benzyl alcohol, ε_{250} = 13,800 M^{-1} cm^{-1}; 280 nm for 2,4-hexadien-1-ol, ε_{280} = 30,140 M^{-1} cm^{-1}. Steady-state kinetics parameters were determined by fitting the initial reactions rates at different substrate concentrations to the Michaelis-Menten equation for one substrate, $v/e = k_{cat}.S/(K_m + S)$ where *e* represent the enzyme concentration, k_{cat} is the maximal turnover rate, S is the substrate concentration and K_m the Michaelis constant. Data were fit using SigmaPlot 10.0 (Systat. Software Inc. Richmond, CA, USA).

2.7.5 Protein modeling

A structural model of the AAO from *P. eryngii* crystal structure at a resolution of 2.55 Å (Protein Data Bank Europe [PDB] accession number 3FIM, (Fernandez et al., 2009) was used as scaffold for the wild type AAO model and the FX9 mutant homology model, obtained by PyMol (Schrodinger LLC.; http://www.pymol.org).

300 **2.7.6 DNA sequencing**

301 All genes were verified by DNA sequencing (BigDye Terminator v3.1 Cycle Sequencing
302 Kit). The primers for the genes cloned in the pJRoC30 plasmid were: primers sense, RMLN and
303 AAOsec1F 5'-GTGGATCAACAGAAGATTTCGATCG-3' and primers antisense RMLC 5'-
304 GCTTACATTCACGCCCTCCC-3', AAOsec2R 5'-GTGGTTAGCAATGAGCGCGG-3' and AAOsec3R 5'-
305 GGAGTCGAGCCTCTGCCCCT-3'. For the AAO genes cloned in the pPICZ-B plasmid primers were:
306 ppKpnAAO-dir and AAOsec1F as primers sense and ppAAO-rev, AAOsec2R and AAOsec3R as
307 primers antisense.

308 **3. RESULTS AND DISCUSSION**

309 **3.1 Improved secretion in *S. cerevisiae* by in vivo shuffling and MORPHING of the chimeric**
310 **signal peptide**

311 During the first evolutionary campaign to increase AAO secretion in yeast, six mutants
312 (carrying 7 beneficial mutations) were identified with improvements in total activity that
313 ranged from roughly 2- up to 100-fold (for $_{Sac}$FX7), **Fig. 1** (Viña-Gonzalez et al., 2015). Given
314 that most of these mutations were >20 residues from one another, they were shuffled in vivo
315 by taking advantage of the homologous recombination machinery of *S. cerevisiae* (Gonzalez-
316 Perez et al., 2012). The mutant library was screened in the HRP-ABTS assay using *p*-
317 methoxybenzyl alcohol as the substrate as described previously (Viña-Gonzalez et al., 2015;
318 Viña-Gonzalez et al., 2016). The best mutant from this round of DNA shuffling was $_{Sac}$FX8,
319 which showed 2.6-fold and 250-fold improved total activity over $_{Sac}$FX7 and the parental AAO,
320 respectively. As planned, several crossover events took place that allowed mutations from
321 different parental types to be convened: the consensus-ancestral mutation H91N from $_{Sac}$FX7;
322 the L170M mutation from $_{Sac}$10G5; and the T50A mutation at the K_1 killer toxin pro-leader
323 inherited from $_{Sac}$12G12, **Fig. 1**. To further enhance secretion, we evolved the preαproK signal
324 leader by MORPHING, a domain-focused mutagenesis technique that allows mutations and

325 crossover events to be randomly introduced in defined stretches (Gonzalez-Perez et al., 2014).
326 With this strategy 3 new mutations were included in the preαproK (F3S at the preα, and H25N-
327 F52L at the K_1 pro-leader), giving rise to the final $_{Sac}$FX9 secretion variant with a 350-fold
328 improvement in activity relative to the parental AAO type and with expression levels of 4.5
329 mg/L in flask culture.

330 The evolved leader sequence of $_{Sac}$FX9 derived from the DNA shuffling and the focused
331 evolution experiments carried four substitutions relative to the original preαproK chimeric
332 construction, **Fig. 1, Fig. 2A**. The preα-leader segment carries the F[3_α]S mutation which agrees
333 well with substitutions at the same position (F[3_α]P/L) previously found in α-factor prepro-
334 leaders that improved antibody secretion (Rakestraw et al., 2009). An acidic residue was
335 introduced into the proK-peptide with the new substitution N[25_K]D, whereas mutation
336 T[50_K]A, inherited from parental type 12G12, together with F[52_K]L increase the hydrophobic
337 load of the middle sequence. In the mature protein, the mutation L170M from the parental
338 10G5 is located in an α-helix at the surface and mutation H91N from FX7 is in the catalytic
339 pocket, **Fig. 2B, C**. As we described previously, Asn91 is a consensus residue situated at the *si-*
340 face of the FAD that stabilizes the conformation of the cofactor, thereby enhancing secretion
341 and AAO stability (Viña-Gonzalez et al., 2015).

342 **3.2 Functional expression of recombinant AAO in *P. pastoris* and scaling-up**

343 The use of compatible tandem-expression systems for protein engineering and
344 overproduction can overcome certain limitations when dealing with complex eukaryotic
345 enzymes like AAO (Alcalde et al., 2015). In particular, combining *S. cerevisiae* as the host of
346 choice for the directed evolution of eukaryotic ligninases with the methylotrophic yeast *P.*
347 *pastoris* (currently reclassified as *Komagataella phaffii*) for overproduction offers many
348 attractive advantages, as demonstrated recently (Mate et al., 2013; Molina-Espeja et al.,
349 2015). Heterologous expression in *S. cerevisiae* and *P. pastoris* falls under the lowest-common-

denominator of a well-defined secretory apparatus and the ability to perform complex post-translational modifications, which frequently results in reasonable secretion of the active and stable enzyme. However, *S. cerevisiae* has a broad variety of episomal vectors, high-transformation efficiencies and a precise recombination apparatus to aid the creation and screening of mutant libraries for directed evolution. While *P. pastoris* lacks such properties, it outperforms *S. cerevisiae* in terms of protein production under the control of strong and tightly regulated promoters, reaching extremely high cell densities in bioreactors (Ahmad et al., 2014). Hence, during the heterologous expression of AAO in yeast, the question that arises is can the improvements in secretion obtained by directed evolution in *S. cerevisiae* be transferred to *P. pastoris*, or in other words, how well are the improvements in secretion preserved in both yeasts.

To assess the compatibility of these two systems, the evolved variants $_{Sac}$FX7 and $_{Sac}$FX9 were cloned into *P. pastoris* to determine if the improvements in secretion furbished by the mutations are consistent between hosts. Under the methanol inducible AOX1 promoter, transformants were grown in deep-well plate microfermentations and screened for secretion - *P. pastoris* can integrate up to six copies of the foreign gene into its genome-. Selected clones, $_{\pi}$FX7 and $_{\pi}$FX9, were then produced in 100 mL shaking flask cultures, producing total activity values of 50 and 235 U/L, respectively. Hence, the beneficial mutations for secretion in *S. cerevisiae* retained their effects in *P. pastoris* and they were even associated with an improvement in total activity from 3.6 to 4.7-fold in both the variants. To harness the high cell titers of *P. pastoris* in the bioreactor, $_{\pi}$FX9 was transferred to a 5L fed-batch fermenter and after six days, maximal volumetric activity was reached (1378 U/L) with the production of AAO (25.5 mg/L) surpassing that obtained in shaking-flask cultures roughly 6-fold. Since AAO is secreted similarly by *S. cerevisiae* and *P. pastoris* (**Table 1**), this improved production can be solely attributed to the high cell densities achieved by *P. pastoris* in the bioreactor (up to 260 g wet biomass/L; $OD_{600} \sim 430$), **Fig. 3A**.

3.3 Influence of glycosylation on biochemical parameters

The $_{Sac}$FX9 and $_{\pi}$FX9 variants were purified to homogeneity and characterized biochemically. N-terminal sequencing confirmed the correct cleavage of the chimeric preαproK by the KEX2 protease in the Golgi compartment in both yeasts, **Table 1**. It is well known that *S. cerevisiae* produces strong glycosylation during heterologous protein expression. Indeed, as occurred with the parental $_{Sac}$FX7 (Viña-Gonzalez et al., 2015), $_{Sac}$FX9 underwent hyperglycosylation (~60% glycosylation) and the wide smear produced by the different glycoforms (ranging from ~200 to 63 kDa in SDS-PAGE) collapsed into a single 63 kDa band after deglycosylation with EndoH, **Fig. 3B, Table 1**. By contrast, in *P. pastoris* the same variant ($_{\pi}$FX9) produced a single ~63 kDa band before and after treatment with EndoH, highlighting the weak glycosylation expected in *P. pastoris*, **Fig. 3B**. The T_{50} (the temperature at which the enzyme retains 50% of its activity after a ten minute incubation) of $_{Sac}$FX9 was slightly higher (1.7°C) than that of $_{\pi}$FX9, possibly due to this hyperglycosylation, **Table 1, Fig. 2C**. As such, the kinetic thermostability of both the recombinant variants expressed by the yeasts exceeded that reported for wild type AAO expressed in *E. coli* after in vitro refolding by ~15 °C (T_{50} = 47.5 °C), emphasizing the beneficial effect of: i) natural folding and heterologous secretion in yeast; and ii) the introduction of the stabilizing consensus-ancestor mutation H91N, as described previously (Viña-Gonzalez et al., 2015). The pH activity profile of $_{Sac}$FX9 and $_{\pi}$FX9 with *p*-methoxybenzyl alcohol was similar, maintaining over 90 % of their activity from pH 2.0 to 6.0, **Fig. 3D**. When the steady kinetic parameters were measured for the oxidation of aromatic and aliphatic alcohols, **Table 2**, the catalytic efficiencies of $_{Sac}$FX9 were similar to those of the parental type $_{Sac}$FX7, as was the order of preference for the different substrates. By contrast, $_{\pi}$FX9 retained similar K_m values to that of $_{Sac}$FX9 but improved by ~2-fold the k_{cat} irrespective of the alcohol tested.

The discrepancies in the kinetic parameters and thermostability between $_{Sac}$FX9 and $_{\pi}$FX9 may be related to the different degrees of glycosylation in *S. cerevisiae* and *P. pastoris*. To assess this, FX9 was also cloned into the glycosylation-deficient Δ*kre2 S. cerevisiae* strain. Δ*kre2* is thought to attach smaller mannose oligomers than wild type strains to the 7 predicted N-glycosylation motifs (Asn-X-Ser/Thrs) in AAO (*i.e.* N62, N138, N151, N222, N303, N325 and N369). After production and purification, the variant secreted by Δ*kre2* ($_{\Delta}$FX9) was characterized biochemically. As predicted, noticeable lower glycosylation was evident by SDS-PAGE, resolving to a smooth smear with a concentration of the protein at ~63 kDa, and it unequivocally tightened into a single band upon deglycosylation, **Fig. 3B, Table 1**. The $_{\Delta}$FX9 variant displayed a similar pH activity profile to its AAO counterparts together with a T_{50} value identical to that of $_{\pi}$FX9 (*i.e*. 1.7°C lower than $_{Sac}$FX9), **Fig. 3C, D**. To complete the breakdown of the biochemical properties of the recombinant AAOs, the kinetic parameters of $_{\Delta}$FX9 were measured. As expected, they came close to those of $_{\pi}$FX9 due to the ~1.5-fold enhancement in the k_{cat} while the K_m was maintained, **Table 2**. Together, the expression of FX9 in Δ*kre2* confirmed that the variation in kinetics and thermostability between $_{Sac}$FX9 and $_{\pi}$FX9 were produced by the distinct degree of glycosylation.

3.4 CONCLUSIONS

This study shows how to harness a tandem-yeast expression system to engineer a fungal AAO by directed evolution and overproduce it in a bioreactor. The properties acquired during the evolution cycles in *S. cerevisiae* are easily decoded by *P. pastoris*, which can produce the recombinant enzyme while retaining its improved catalytic properties and general stability. As a natural progression, future studies could focus on the production of the recombinant enzyme at the g/L scale in other strong industrial hosts like *Trichoderma* or *Aspergillus sp.* Certainly, the findings presented here invite a further exploration and extension of the biotechnological potential of AAO, for example tailoring its activity to oxidize secondary

alcohols and resolve chiral mixtures, or tuning the AAO catalysis to furfural-derivative cascade reactions (Hernandez-Ortega et al., 2012b; Carro et al., 2015; Martinez et al., 2017).

ACKNOWLEDGEMENTS

This research was supported by the EU project FP7-KBBE-2013-7-613549-INDOX and by the Spanish Government project BIO2016-79106-R-Lignolution.

REFERENCES

Alcalde, M. (2015). Engineering the ligninolytic enzyme consortium. *Trends in Biotechnology*, **33**, 155-162. DOI: 10.1016/j.tibtech.2014.12.007

Ahmad, M., Hirz, M., Pichler, H., & Schwab, H. (2014). Protein expression in *Pichia pastoris*: recent achievements and perspectives for heterologous protein production. *Applied Microbiology and Biotechnology,* **98**, 5301–5317. DOI: 10.1007/s00253-014-5732-5

Carro, J., Ferreira, P., Rodriguez, L., Prieto, A., Serrano, A., Balcells, B., … & Martinez, A.T. (2015). 5-hydroxymethylfurfural conversion by fungal aryl-alcohol oxidase and unspecific peroxygenase. *FEBS Journal* **282**, 3218-3229. DOI: 10.1111/febs.13177

Fernandez, I.S., Ruiz-Dueñas, F.J., Santillana, E., Ferreira, P., Martinez, M.J., Martinez, A.T., & Romero, A. (2009). Novel structural features in the GMC family of oxidoreductases revealed by the crystal structure of fungal aryl-alcohol oxidase. *Acta Crystallographica Section D*, **65**, 1196-1205. DOI: 10.1107/S0907444909035860

Ferreira, P., Medina, M., Guillén, F., Martínez, M. J., Van Berkel, W.J, & Martínez, AT. (2005). Spectral and catalytic properties of aryl-alcohol oxidase, a fungal flavoenzyme acting on polyunsaturated alcohols. *Biochemical Journal*, **389**, 731–738. DOI: 10.1042/BJ20041903

Gonzalez-Perez, D., Garcia-Ruiz, E., & Alcalde, M. (2012). *Saccharomyces cerevisiae* in directed evolution: an efficient tool to improve enzymes. *Bioengineered*, **3**, 1-6. DOI: 10.4161/bbug.19544

450 Gonzalez-Perez, D., Molina-Espeja, P., Garcia-Ruiz, E. & Alcalde, M. (2014). Mutagenic
451 organized recombination process by homologous in vivo grouping (MORPHING) for directed
452 enzyme evolution, *PLoS One*. 9:e90919. DOI: 10.1371/journal.pone.0090919

453 Hernandez-Ortega, A., Ferreira, P. & Martinez, A.T. (2012a). Fungal aryl-alcohol oxidase: a
454 peroxide-producing flavoenzyme involved in lignin degradation. *Applied Microbiology and*
455 *Biotechnology*, **93**, 1395-1410. DOI: 10.1007/s00253-011-3836-8

456 Hernandez-Ortega, A., Ferreira, P., Merino, P., Medina, M., Guallar, V. & Martinez, A.T.
457 (2012b). Stereoselective hydride transfer by aryl-alcohol oxidase, a member of the GMC
458 superfamily. *ChemBioChem*, **13**, 427-435. DOI: 10.1002/cbic.201100709

459 Lin-Cereghino, J., & Cregg, J.M. (2000). Heterologous protein expression in the methylotrophic
460 yeast *Pichia pastoris*. *FEMS Microbiology Reviews*, **24**, 45–66. DOI: 10.1111/j.1574-
461 6976.2000.tb00532.x

462 Martinez, A.T., Ruiz-Dueñas, F.J., Camarero, S., Serrano, A., Linde, D., Lund, H., … & Alcalde, M.
463 (2017). Oxidoreductases on their way to industrial biotransformations. *Biotechnology*
464 *Advances*, **35**, 815-831. DOI: 10.1016/j.biotechadv.2017.06.003

465 Martinez, A.T., Ruiz-Dueñas, F.J., Martínez, M.J., del Río, J.C., & Gutierrez, A. (2009). Enzymatic
466 delignification of plant cell wall: from nature to mill. *Current Opinion in Biotechnology*, **20**,
467 348–357. DOI: 10.1016/j.copbio.2009.05.002

468 Mate, D., Gonzalez-Perez, D., Kittl, R., Ludwig, R. & Alcalde M. (2013). Functional expression of
469 a blood tolerant laccase in *Pichia pastoris*. *BMC Biotechnology*, **13**, 38. DOI: 10.1186/1472-
470 6750-13-38

471 Molina-Espeja, P., Ma, S., Mate, D.M., Ludwig, R. & Alcalde, M. (2015). Tandem-yeast
472 expression system for engineering and producing unspecific peroxygenase. *Enzyme and*
473 *Microbial Technology*, **73-74**, 29-33. DOI: 10.1016/j.enzmictec.2015.03.004

474 Nothwehr, S.F., & Gordon, J.I. (1990). Structural features in the N_{H2}-terminal region of a model
475 eukaryotic signal peptide influence the site of its cleavage by signal peptidase. *Journal of*
476 *Biological Chemistry*, **265**, 17202-8.

477 Rakestraw, J.A., Sazinsky, S.L., Piatesi, A., Antipov, E., & Wittrup, K.D. (2009). Directed
478 evolution of a secretory leader for the improved expression of heterologous proteins and full-
479 length antibodies in *Saccharomyces cerevisiae*. *Biotechnology and Bioengineering,* **103**, 1192-
480 201. DOI: 10.1002/bit.22338

481 Viña-Gonzalez, J., Gonzalez-Perez, D., Ferreira, P., Martinez, A.T. & Alcalde, M. (2015). Focused
482 directed evolution of aryl-alcohol oxidase in yeast by using chimeric signal peptides. *Applied*
483 *and Environmental Microbiology*, **81**, 6451-6462. DOI: 10.1128/AEM.01966-15

484 Viña-Gonzalez, J., Gonzalez-Perez, D., & Alcalde, M. (2016). Directed evolution method in
485 *Saccharomyces cerevisiae*: Mutant library creation and screening. *Journal of Visualized*
486 *Experiments*, 110: e53761. DOI: 10.3791/53761

487

488

489

490

491

492

493

494

495

496

497 **FIGURE LEGENDS**

498 **Figure1.** Laboratory evolution of the AAO from *Pleurotus eryngii* towards functional expression
499 in yeast. New mutations are represented as stars and accumulated mutations as squares. The
500 preα-leader segment is depicted in green, the prok-leader segment in light blue and the
501 mature AAO in dark blue. The TAI (total activity improvement) is the value indicating the
502 improvement in AAO activity detected in *S. cerevisiae* supernatants relative to the parental
503 type: *1^{st} G, results from the first generation of variants published in Viña-Gonzalez et al.,
504 2015.

505 **Figure 2.** Mutations presented by FX9. (**A**) Substitutions in the chimeric preαproK signal
506 peptide. (**B** and **C**) Molecular model using the *Pleurotus eryngii* AAO crystal structure as a
507 template (PDB code 3FIM). (**B**) wild type AAO and (**C**) the FX9 variant. FAD is depicted in yellow
508 and the details of the two mutations in FX9 (blue) are compared with the corresponding
509 residues in the wild type (red).

510 **Figure 3.** (**A**) Fermentation in a 5L bioreactor of recombinant $_{\pi}$FX9 expressed in *P. pastoris*.
511 Fermentation was performed in four steps: glycerol-batch phase for 26 h, glycerol-fed phase
512 for 4h, transition phase for 4 h and methanol induction phase for 112 h. The black circles
513 represent the wet biomass, the white triangles the volumetric AAO activity and the dotted
514 vertical line the beginning of the induction phase. (**B**) Molecular mass of recombinant AAO.
515 10% SDS-polyacrylamide gel: Lanes 1 and 8, protein markers; 2, purified $_{sac}$FX9 mutant; 3,
516 deglycosylated $_{sac}$FX9; 4, purified $_{\Delta}$FX9; 5, deglycosylated $_{\Delta}$FX9; 6, purified $_{\pi}$FX9; 7
517 deglycosylated $_{\pi}$FX9. (**C**) Kinetic thermostability (T_{50}) of the recombinant variants: $_{sac}$FX9 (grey
518 triangles), $_{\Delta}$FX9 (black squares) and $_{\pi}$FX9 (white circles). (**D**) pH activity profiles for $_{sac}$FX9 (grey
519 triangles), $_{\Delta}$FX9 (black squares) and $_{\pi}$FX9 (white circles) with *p*-methoxybenzyl alcohol (1 mM).
520 Each point represents the mean and standard deviation of three independent experiments.

521

TEXT FOR GRAPHICAL TABLE OF CONTENTS:

Fungal aryl-alcohol oxidases (AAO) are precious biocatalysts whose presence in industrial biotechnology is being impeded by the absence of proper heterologous expression system. In the present study, the functional expression of AAO from white rot fungus *Pleurotus eryngii* was adapted to a tandem-yeast expression system aimed at boosting secretion. After applying different directed evolution strategies in *S. cerevisiae*, the evolved AAO was successfully overproduced in *Pichia pastoris* in bench-bioreactor.

Figure 1

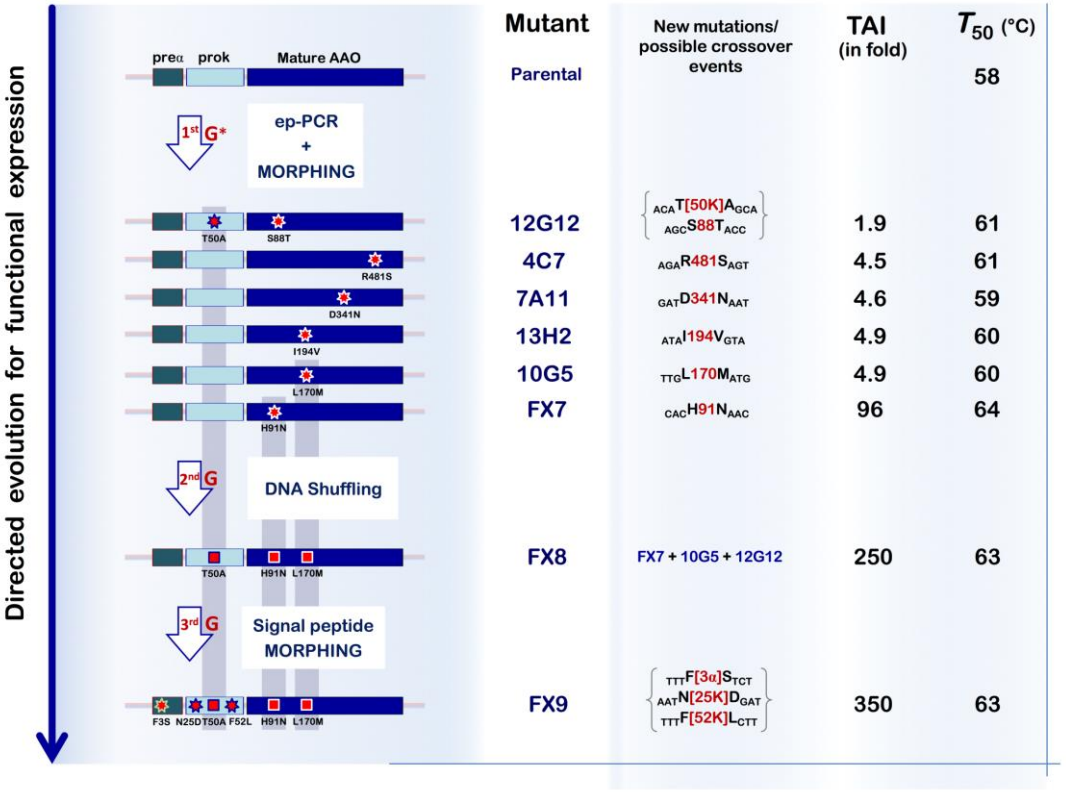

532

Figure 2

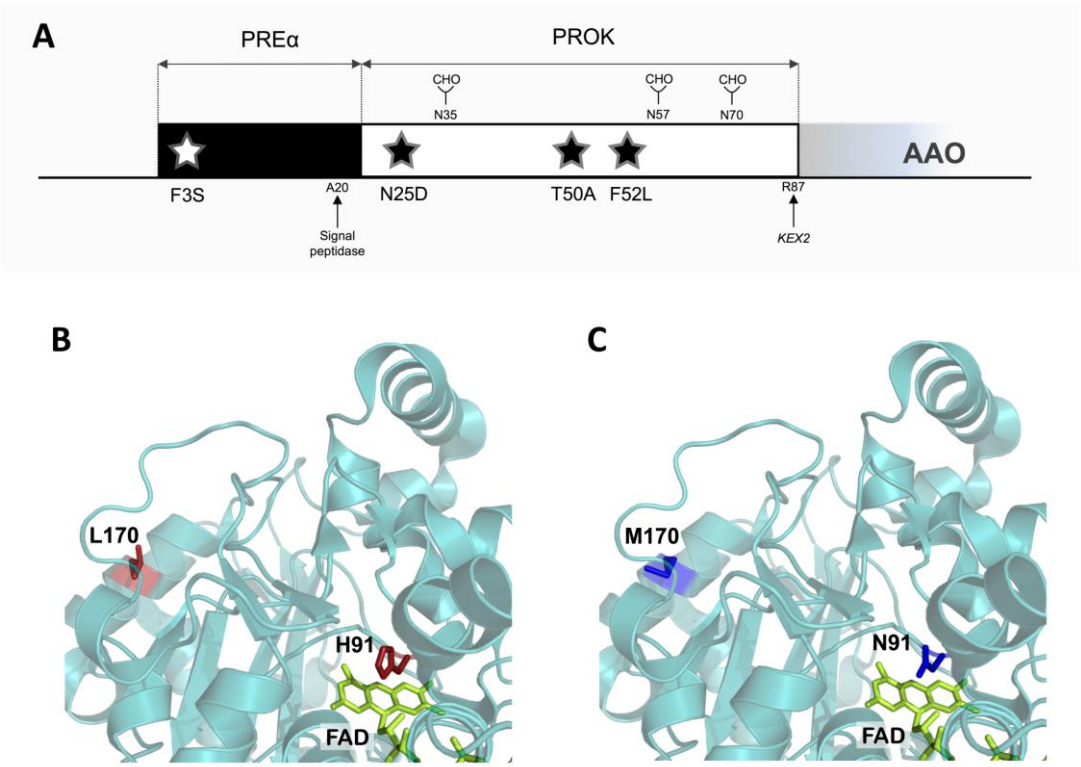

533

Figure 3

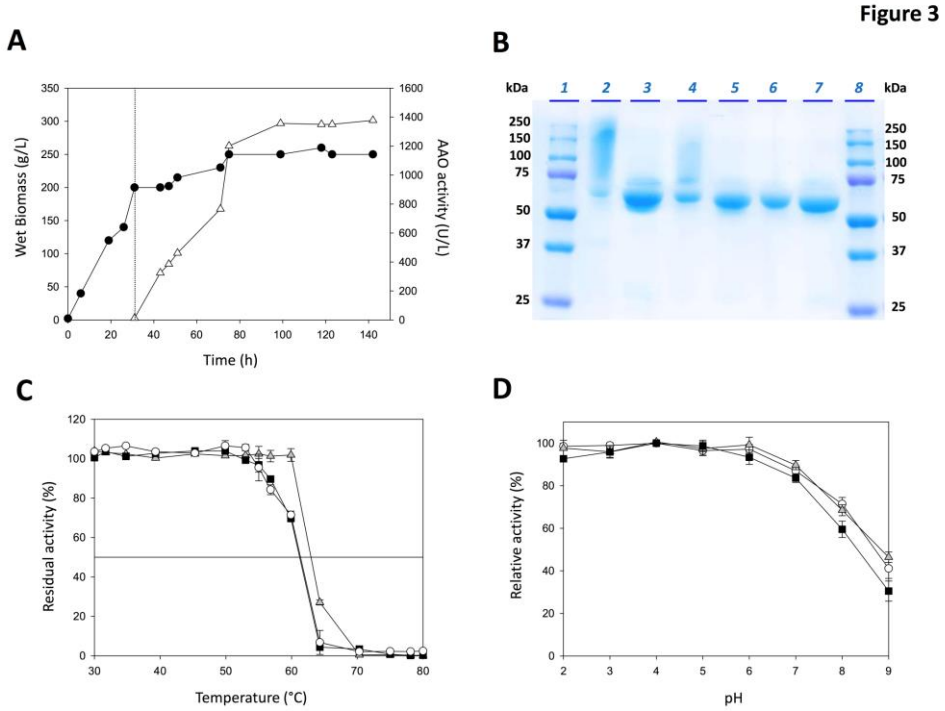

534

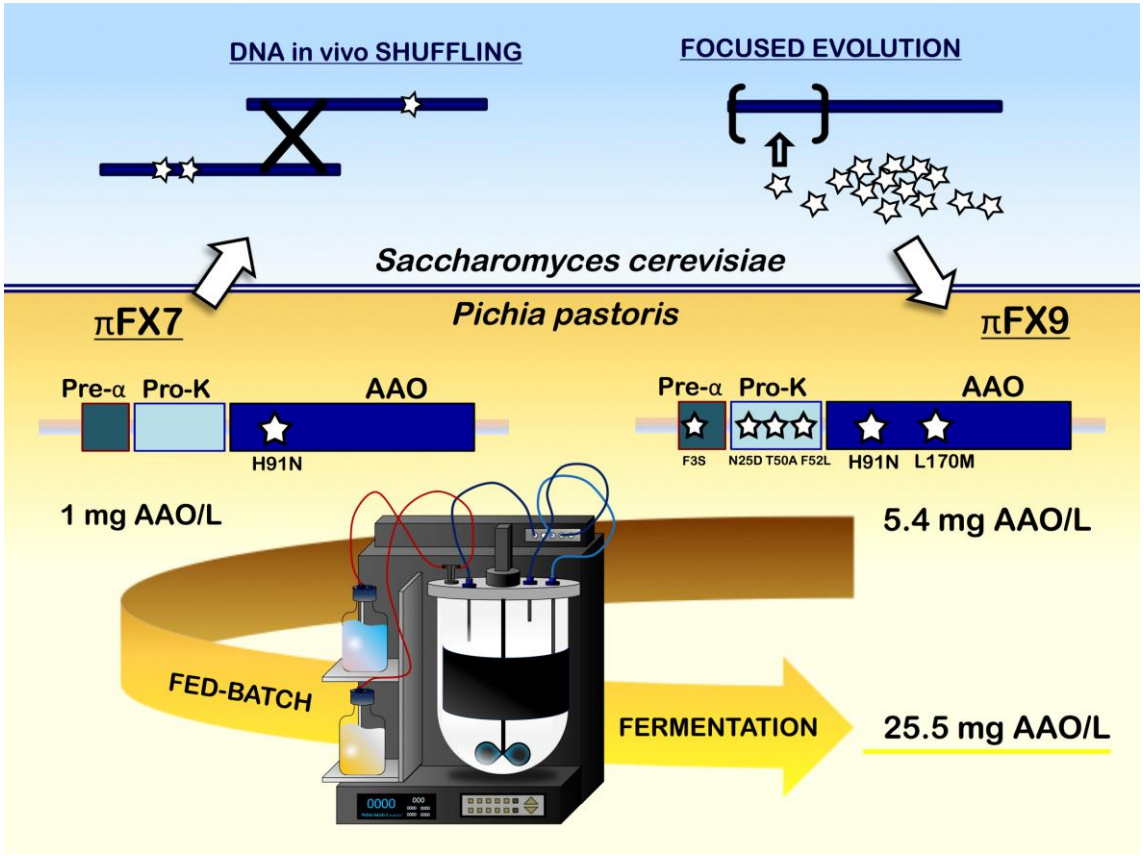

535